NJC

ROYAL SOCIETY OF CHEMISTRY

PAPER

View Article Online
View Journal | View Issue

Cite this: *New J. Chem.*, 2024, **48**, 4931

Modifying the terminal phenyl group of monomethine cyanine dyes as a pathway to brighter nucleic acid probes†

Johanna M. Alaranta, [a] Arto M. Valkonen, [a] Sailee S. Shroff, [b] Varpu S. Marjomäki, [b] Kari Rissanen [a] and Tanja M. Lahtinen *[a]

Received 23rd November 2023,
Accepted 19th February 2024

DOI: 10.1039/d3nj05400d

rsc.li/njc

Three novel monomethine cyanine dyes were synthesized carrying electron donating groups to obtain even brighter nucleic acids probes. Photophysical properties of these dyes were evaluated with DNA and selected dyes with RNA. A great variation in brightness and binding properties of the dyes was observed. Moreover the X-ray crystal structures are presented for two dyes.

Fluorescent probes are an essential part of the molecular biologist's instrumentation to image nucleic acids in a wide range of applications. These include for example PCR,[1–5] melting curve analysis,[6,7] quantification of nucleic acids from environmental samples[8] and gel electrophoresis.[9] A widely utilized probe for these applications is, for example, **SYBR Green I**, which has been very popular since it was introduced.[10] Monomethine cyanine dyes exhibit all the expected qualities for excellent fluorescent probes for nucleic acids: turn-on fluorescence with low background emission, desirable photostability and they are less toxic to cells when compared to another popular DNA stain, ethidium bromide.[11] However, during recent years the demand for selective dyes for different types of nucleic acids has increased. The increasing interest to study RNA, for example to the develop antivirals[12] and RNA vaccines,[13] has only amplified the appeal to research RNA specific fluorescent probes. Also designing even more sensitive dyes to accommodate the new challenging applications, such as studying the opening mechanism of viruses is equally important.[14] By understanding the structural elements underlying the biological activity of these dyes, is one possible way to achieve these goals.

In recent years we have systematically studied the structure of SYBR green related cyanine dyes, trying to find the key points that change the photophysical qualities of these dyes. 14 newly synthesized monomethine cyanine dyes and their structural differences and their effect to the photophysical qualities have been studied by us.[14–16] The goal is to identify the important elements, so that the best structural features can be combined to produce the ultimate fluorescent probe for nucleic acid staining. In our previous studies, the binding properties were investigated for all 14 dyes with DNA and for selected dyes, also with RNA, to understand the phenomena behind the great turn-on fluorescence. The molecular modelling indicated that the dyes synthesised by us bind in the minor groove of the DNA double helix, while it had been widely accepted that SYBR Green related dyes are mainly intercalators.[17,18] It was also shown that one way to improve the brightness of the dyes could be by enhancing the rigidity of the molecule when binding the dsDNA. We also noted that the heteroatoms in different positions of the dye core had great effect to the photophysical qualities and just by changing one heteroatom, for example oxygen to sulphur, clear difference in these qualities could be observed. The effect of heteroatoms on the photophysical qualities have intrigued many scientists working in the wide field of fluorescent probes, such as rhodamines,[21] which has been extensively studied as well as difluoroborates.[22] Moreover, all our dyes have had highest molar absorption coefficients in ethanol or DCM where the dyes are fully soluble.[14,15] Kurutos *et al.*[23] have previously showed that one way to improve monomethine cyanine dyes qualities and make them more user friendly is to improve the water solubility by adding substituents to alkyl chains with additional charges to the main core of the dyes.

With all these results in mind, we designed modifications for the terminal phenyl group in a way that aims to improve the binding rigidity and/or the water solubility of these dyes (Fig. 1). As we had a demonstrated earlier, we had a core structure of **OxN (4)** which already has many of the desired qualities for a fluorescent probe – good quantum yield, photostability even in prolonged studies, strong binding with DNA

[a] *University of Jyväskylä, Department of Chemistry, Nanoscience Centre, P.O. Box 35, Jyväskylä, FI-40014, Finland. E-mail: tanja.m.lahtinen@jyu.fi*
[b] *University of Jyväskylä, Department of Cell and Molecular Biology, Nanoscience Centre, Jyväskylä, FI-40014, Finland*

† Electronic supplementary information (ESI) available: Experimental details, detailed synthesis methods, product characterizations, comprehensive photophysical studies, including binding studies including dyes and dsDNA. CCDC 2294210 and 2294211. For ESI and crystallographic data in CIF or other electronic format see DOI: **https://doi.org/10.1039/d3nj05400d**

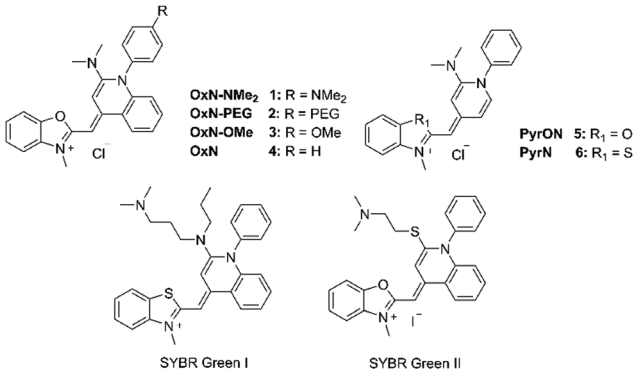

Fig. 1 Novel dyes **1–3** compared to previously published dyes **4–6**[16] and commercial dyes **SYBR Green I**[10,19] and **SYBR Green II**.[14,20]

and great turn-on fluorescence with low background emission. By further modifying this core we wanted to achieve two goals: increase the water solubility along with binding affinity and to gain more understanding how these structural modifications change the photophysical properties of the dyes.

Dimethylamine as a substituent was obvious choice since we had already seen that it improves the binding and brightness compared to thiol[15,16] and since it its capable of hydrogen bonding with the lone pair electrons, it could also improve the water solubility and at the same time enhance the binding affinity with the DNA. PEG group was included to for certain to see if the water solubility could be the answer to brighter and perhaps more user-friendly usage. Since **OxN-PEG** has the outreaching oxyethylene chain, we also wanted to include control of just methoxy group to see if the length of PEG chain affects the binding properties.

Dyes **1–3** were synthesized by using previously published methods.[14,15,24] The dye synthesis were done using the cyanine condensation method with quinoline salt and benzoxazolium salt as starting materials. In inert conditions, using triethylamine as a base catalyst, condensation is achieved in room temperature within four hours. Our synthesis also has additional substitution step to replace chloride in the quinoline moiety with dimethylamine. Purification is done with flash column chromatography, which are usually done at least twice to achieve desired purity. PEGylation of 4-iodophenol was done according to procedure by Nguyen *et. al.*[25] Detailed synthesis routes along with X-ray crystal structure parameters and geometry calculations can be found in ESI.†

Suitable crystal quality for single crystal X-ray diffraction (SCXRD) analysis were obtained from **1** and **3**. The crystal data and other experimental details for dyes **1** and **3** are given in the ESI.† As observed with the related dyes in our previous study,[16] the main molecular skeletons of **1** and **3** including benzoxazolium and quinoline moieties are planar in the solid state (Fig. S15 and S16, ESI†). The overall structures are also very similar to the quinoline containing dyes previously described by us.[16] The most notable deviation from the planarity of the entire molecules is observed with the phenyl ring bonded to quinoline nitrogen. The plane of the phenyl ring shows angles of 67.0° in **1** and of 71.6° (72.7°, 2nd molecule) in **3** to the plane of the dye skeleton. The high-level DFT [M06-2X, def2-TZVP with acetonitrile (dielectric = 37.50] as a solvent using C-PCM model) calculations match extremely well with the SCXRD geometry of **OxN-NMe$_2$ (1)**, **OxN-OMe (3)** and previously[16] studied dye **PyrON (5)** (Fig. S19, ESI†).

For absorption, emission, and excitation maxima (Fig. S22 and S23, ESI†), only few nanometre shifts between the dyes **1–3** are seen, essentially, all new dyes have similar maxima as the core dye **OxN (4)**. This is also observed with Stoke's shifts, the shifts only vary from 29 to 34 nm (Table 1). Previously, we had observed that even small, one heteroatom changes in the chromophore could change these maxima drastically in the nanometre scale.

Molar absorption coefficients (ε) were measured in three different solvents, ethanol, tris-EDTA (TE) buffer and 100 μM ct DNA in TE buffer solution. To investigate if the binding with DNA alters the absorption coefficient of the dyes, TE buffer was used as a reference for the final ctDNA solution. Ethanol was chosen as organic solvent to investigate the effect of solubility to the absorption coefficients. All dyes (**1–4**) have the highest absorption coefficients in ethanol (Table 1), following the trend previously observed.[15,16] Interestingly, **OxN-NMe$_2$ (1)** and **OxN-PEG (2)** have the lowest absorption coefficients in TE buffer. This could potentially indicate that without DNA in solution, dyes can for example aggregate, which is known quality of cyanine dyes,[26] lowering the absorption coefficients. While DNA offers favorable binding site where the dyes can fit, preventing the aggregation from happening and the dyes having higher absorption coefficients in ctDNA solution.

Table 1 Photophysical and binding parameters of the studied dyes. Full details of the measurements can be found in ESI

Dye	**OxN (4)**	**OxN-NMe$_2$ (1)**	**OxN-PEG (2)**	**OxN-OMe (3)**	**SYBR Green I**
λ_{abs} (nm)	464	462	463	463	497
ε_{max} (TE buffer) M^{-1} cm^{-1}	56 500 ± 800	52 500 ± 400	13 300 ± 200	51 000 ± 900	73 000[10]
ε_{max} (Ethanol) M^{-1} cm^{-1}	73 600 ± 600	93 000 ± 400	26 900 ± 150	77 900 ± 300	43 300
ε_{max} (100 μM ctDNA) M^{-1} cm^{-1}	47 300 ± 200	61 600 ± 1005	20 300 ± 200	49 800 ± 500	29 500
λ_{emi} (nm)	492	496	493	492	520
Stoke's shift (nm cm^{-1})	28/1230	34/1480	30/1310	29/1270	23/890
Φ	~1	0.014	~1	~1	0.8[19]
Brightness (M^{-1} cm^{-1})	**47 300**	**868**	**20 300**	**49 800**	**34 640**
K_a ($\times 10^6$ M^{-1})	8.5 ± 1.50	0.2 ± 0.02	57.9 ± 3.00	12.8 ± 1.10	5.9 ± 0.05
K_d (nM)	118	4100	17.3	78.1	167
n	3.4 ± 0.40	4.7 ± 0.30	6.0 ± 0.30	3.9 ± 0.09	3.2 ± 0.11
ΔG^0 (kJ mol^{-1})	−39.0	−27.7	−43.1	−41.2	−38.0

OxN-NMe$_2$ (1) and **OxN-OMe (3)** both had excellent absorption coefficients across all media, especially **OxN-NMe$_2$ (1)** having highest value of 93 000 M^{-1} cm^{-1} in ethanol. While **OxN-PEG (2)** did not excel with the absorption coefficients, including PEG arm did not completely shut down the absorption of the dye. Surprisingly, no clear evidence could be observed for the PEG increasing water solubility in UV-vis measurements.

Quantum yields of the dyes were determined with fluorescein standard (Fig. S25, ESI†) to gain more knowledge how the dyes perform when fully bound with ctDNA. Since all experiments so far gave consistent results between the dyes, same was expected for quantum yields. **OxN-PEG (2)** and **OxN-OMe (3)** do follow the trend, since the quantum yield was determined to be **1** for both dyes matching the quantum yield of **OxN (4)**. Surprisingly, the quantum yield of **OxN-NMe$_2$ (1)** was only 0.014 meaning that the additional amine group at the terminal phenyl group significantly quenched the fluorescence intensity of **OxN-NMe$_2$ (1)** when binding ctDNA. This result indicates that this additional electron donating group may alter the relaxation method of the dye after excitation.

Selected dyes (**1**, **3–6** and **SYBR Green I** and **II**) were also studied with RNA, to evaluate their performance compared to DNA. In this study, dye concentrations were kept at 0.05 μm in either DNA solution with concentration of 4.9 ng μl^{-1} or in RNA solution with concentration of 4.4 ng μl^{-1}, respectively. As we can see from Fig. 2, The new dye **OxN-OMe (3)** performs best with DNA, and almost as good as **OxN (4)** with RNA. Interestingly, the **OxN-NMe$_2$ (1)** performed very poorly with both DNA and RNA. **OxN-OMe (3)** and **OxN (4)** outperformed both commercial dyes, **SYBR Green I** and **II** as they have higher normalized emission values with DNA. **OxN (4)** and **OxN-OMe (3)** have slightly higher exaltation (ratio of intensity) with RNA than **SYBR Green II**, but the intensities are quite similar. **PyrON (5)** and **PyrN (6)** presented in our previous studies,[16] have significantly lower exaltation compared to the commercial dyes **SYBR Green I** and **II**, but a slight preference could be seen – **PyrON (5)** has higher exaltation with DNA and **PyrN (6)** with RNA, respectively. The only structural difference between these two is the change from oxazolium (**PyrON (5)**) to thiazolium moiety (**PyrN (6)**). Hence, with one heteroatom change from oxygen to sulfur, we can observe significant change in the photophysical qualities. When dyes have oxygen moiety, benzoxazolium, they seem to prefer DNA over RNA and when dyes have sulfur, benzothiazolium moiety in this study, they seem to prefer RNA. **SYBR Green II** also has the same thiazolium moiety as **PyrN (6)**, hinting that the sulfur might be a possible key element in synthesizing RNA selective dye. To support this theory Lu *et al.*[27] presented an RNA targeting dye with also thiazolium moiety combined with additional thiol substituent.

The binding properties of the dyes were evaluated using McGhee Von Hippel equation (Fig. S24, ESI†).[28] Due to the poor quantum yield of the **OxN-NMe$_2$ (1)**, it was also suspected to bind poorly with the ctDNA. This hypothesis was confirmed in our studies since the binding constant (K_a) was only 0.2×10^6 while previously synthesized **OxN (4)** has had the highest binding constant so far of 8.5×10^6, indicating that the **OxN-NMe$_2$ (1)** has relatively loose binding with the ctDNA compared to previously seen values. However, **OxN-OMe (3)** and especially **OxN-PEG (2)** shows even higher binding affinities than **OxN (4)** and **SYBR Green I**. **OxN-OMe (3)** has binding constant of 12.8×10^6 but **OxN-PEG (2)** is in other level compared to rest of the dyes; it has binding constant of 57.6×10^6. This result indicates that the oxygen rich functional sidechain enhances the binding, which could already be seen for the short methoxy chain in **OxN-OMe (3)**. Binding site sizes (n) for **OxN-NMe$_2$ (1)** and **OxN-OMe (3)** are in same level than to **OxN (4)** which has binding site size 3.4, **OxN-NMe$_2$ (1)** binding site size being 4.7 and **OxN-OMe (3)** 3.9, respectively. Both dyes having slightly larger binding sites due to the additional

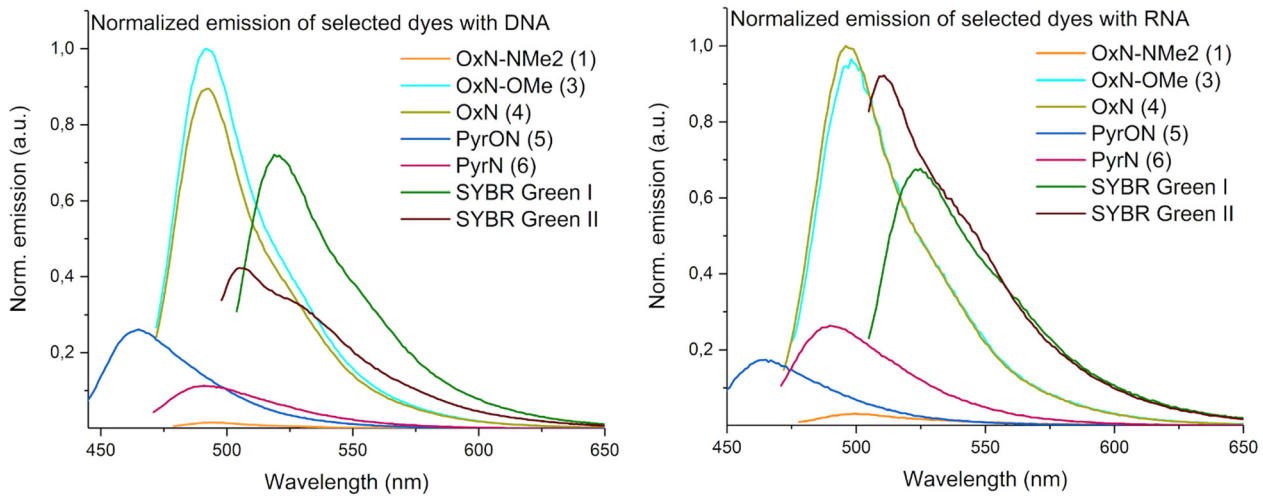

Fig. 2 Normalized emissions of studied dyes with DNA and RNA. The plots are normalized with the emission intensity of the highest emitting dye, **OxN-OMe** for DNA and **OxN** for RNA, to allow comparison of possible trends. For each measurement, dye concentrations were 0.05 μM. Nucleic acid solutions were prepared in TE buffer where DNA concentration was 4.9 ng μl^{-1} and RNA concentration was kept at 4.4 ng μl^{-1}, respectively.

functional groups in the terminal phenyl group. Similarly, **OxN-PEG (2)** has noticeably larger binding site size of 6.0 due to the longer side chain.

Finally, to have one number to compare the dyes, brightness was calculated for each dye by multiplying absorption coefficient in ctDNA solution with the determined quantum yield. This value estimates how many of the absorbed photons can eventually be emitted, hence giving a single value how well the dye can perform as fluorescent probe. Due to the low quantum yield, **OxN-NMe$_2$ (1)** has the lowest brightness of 868 M^{-1} cm^{-1} even though it had the highest absorption coefficient when bound with ctDNA. Great quantum yield and high absorption coefficient of **OxN-OMe (3)** makes it slightly brighter than **OxN (4)** and commercial dye **SYBR Green I** with brightness of 49 800 M^{-1} cm^{-1}. Similar methoxy group enhancement was also observed with indole-based copper probes[29] and tuning thiazole orange with electron donor and acceptor.[30] **OxN-PEG (2)** lands right in the middle, having great quantum yield, but the PEG group lowering the absorption coefficient even though it binds remarkably strongly with ctDNA.

To conclude, three new monomethine cyanine dyes with additional functional groups at the terminal phenyl group were synthesized and compared to the commercial dyes **SYBR Green I** and **II** and to selection of our previously published ones. Effect of different electron donating groups at terminal phenyl group to the photophysical properties were investigated. X-ray crystal structures were solved for **OxN-NMe$_2$ (1)** and **OxN-OMe (3)**. Methoxy (**OxN-OMe (3)**) increased the molar absorption coefficient and emission compared to the dye without any functional group at the same position (**OxN (4)**). However, including amine at this position (**OxN-NMe$_2$ (1)**), did increase the molar absorption coefficient of the dye, but it also quenched the emission intensity almost completely since the quantum yield dropped from 1 to only 0.014. Similarly, also the binding properties of **OxN-NMe$_2$ (1)** dropped significantly compared to other dyes. Interestingly, **OxN-PEG (2)** seems to bind extremely tightly with ctDNA compared to other studied dyes. The PEG substituent could provide additional binding interactions due to the oxygen lone pair electrons in the PEG chain which could interact with the DNA double helix, as observed by Howerton *et al.*[31]

In the end, we were able to design new and even better dye with excellent photophysical properties, **OxN-OMe (3)** exhibiting brightness of 49 800 M^{-1} cm^{-1}, quantum yield ~1 and tight binding with ctDNA. Noting that **OxN-OMe (3)** is also significantly brighter than commercially available **SYBR Green I** with brightness 34 600 M^{-1} cm^{-1}. In this paper we also demonstrated that **OxN (4)** and **OxN-OMe (3)** are excellent choices to image viral RNA, even though they are not selective towards DNA or RNA, but they are more sensitive than the commercially available **SYBR Green II**, which prefers RNA. Additionally compared to other popular nucleic acid stains, ethidium bromide and YOYO-1, our dyes **OxN (4)** and **OxN-OMe (3)** exhibit higher quantum yields and brightness as well as better quantum yield than TOTO-1.[32] It is also noted that including sulphur to the dyes seemed to shift their preference from DNA towards RNA. We believe **OxN-OMe (3)** with additional electron donating group is excellent choice to image nucleic acids in future since it is very sensitive with both ctDNA and RNA. This researched also revealed extremely valuable information about how small changes of the functional groups outside the main chromophore can have drastic effects to the photophysical properties of the dyes.

Author contributions

Johanna Alaranta: writing – original draft, investigation, formal analysis, data curation. Arto Valkonen: data curation, writing – original draft, formal analysis. Sailee Shroff – data curation. Varpu Marjomäki – supervision, investigation. Kari Rissanen: supervision, data curation, formal analysis, writing – original draft. Tanja Lahtinen: writing – original draft, data curation, formal analysis, investigation, funding acquisition, project administration.

Conflicts of interest

There are no conflicts to declare.

Acknowledgements

Authors thank Dr Tatu Kumpulainen for his assistance with the spectroscopy studies. Kari Rissanen gratefully acknowledge the Academy of Finland (grant number: 351121).

Notes and references

1 F. Ponchel, C. Toomes, K. Bransfield, F. T. Leong, S. H. Douglas, S. L. Field, S. M. Bell, V. Combaret, A. Puisieux, A. J. Mighell, P. A. Robinson, C. F. Inglehearn, J. D. Isaacs and A. F. Markham, *BMC Biotechnol.*, 2003, **3**, DOI: 10.1186/1472-6750-3-18.
2 N. Marmiroli and E. Maestri, in *Food Toxicants Analysis*, Elsevier, 2007, ch. 6, pp. 147–187.
3 H. Cao and J. M. Shockey, *J. Agric. Food Chem.*, 2012, **60**, 12296–12303.
4 M. Bengtsson, H. J. Karlsson, G. Westman and M. Kubista, *Nucleic Acids Res.*, 2003, **31**, e45.
5 D. R. Marinowic, G. Zanirati, F. V. F. Rodrigues, M. V. C. Grahl, A. M. Alcará, D. C. Machado and J. C. Da Costa, *Sci. Rep.*, 2021, **11**, 2224.
6 J. S. Farrar and C. T. Wittwer, in *Molecular Diagnostics*, Elsevier, 2017, pp. 79–102.
7 K. M. Ririe, R. P. Rasmussen and C. T. Wittwer, *Anal. Biochem.*, 1997, **245**, 154–160.
8 H. Zipper, C. Buta, K. Lämmle, H. Brunner, J. Bernhagen and F. Vitzthum, *Nucleic Acids Res.*, 2004, **32**, e103.
9 A. E. Kiltie and A. J. Ryan, *Nucleic Acids Res.*, 1997, **25**, 2945–2946.
10 H. Zipper, H. Brunner, J. Bernhagen and F. Vitzthum, *Nucleic Acids Res.*, 2004, 32.

11 K. I. Kirsanov, E. A. Lesovaya, M. G. Yakubovskaya and G. A. Belitsky, *Mutat. Res., Genet. Toxicol. Environ. Mutagen.*, 2010, **699**, 1–4.
12 M. Laajala, K. Kalander, S. Consalvi, O. S. Amamuddy, Ö. T. Bishop, M. Biava, G. Poce and V. Marjomäki, *Pharmaceutics*, 2023, 15.
13 N. Pardi, M. J. Hogan, F. W. Porter and D. Weissman, *Nat. Rev. Drug Discovery*, 2018, **17**, 261–279.
14 V. K. Saarnio, K. Salorinne, V. P. Ruokolainen, J. R. Nilsson, T. R. Tero, S. Oikarinen, L. M. Wilhelmsson, T. M. Lahtinen and V. S. Marjomäki, *Dyes Pigm.*, 2020, **177**, 108282.
15 V. K. Saarnio, J. M. Alaranta and T. M. Lahtinen, *J. Mater. Chem. B*, 2021, **9**, 3484–3488.
16 J. M. Alaranta, K.-N. Truong, M. F. Matus, S. A. Malola, K. T. Rissanen, S. S. Shroff, V. S. Marjomäki, H. J. Häkkinen and T. M. Lahtinen, *Dyes Pigm.*, 2022, **208**, 110844.
17 A. I. Dragan, R. Pavlovic, J. B. McGivney, J. R. Casas-Finet, E. S. Bishop, R. J. Strouse, M. A. Schenerman and C. D. Geddes, *J. Fluoresc.*, 2012, **22**, 1189–1199.
18 A. I. Dragan, J. R. Casas-Finet, E. S. Bishop, R. J. Strouse, M. A. Schenerman and C. D. Geddes, *Biophys. J.*, 2010, **99**, 3010–3019.
19 Invitrogen. SYBR ® green I nucleic acid gel stain product information sheet, vols. 1–5, 2006.
20 SYBR® Green II RNA Gel Stain, Molecular Probes, 2001.
21 F. Deng and Z. Xu, *Chin. Chem. Lett.*, 2019, **30**, 1667–1681.
22 A. M. Grabarz, B. Jędrzejewska, A. Skotnicka, N. A. Murugan, F. Patalas, W. Bartkowiak, D. Jacquemin and B. Ośmiałowski, *Dyes Pigm.*, 2019, 170.
23 A. Kurutos, I. Balabanov, F. S. Kamounah, K. Nikolova-Ganeva, D. Borisova, N. Gadjev, T. Deligeorgiev and A. Tchorbanov, *Dyes Pigm.*, 2018, **157**, 267–277.
24 L. Ying, *US Pat.*, US20130137875A1, 2013.
25 R. Nguyen, N. Jouault, S. Zanirati, M. Rawiso, L. Allouche, G. Fuks, E. Buhler and N. Giuseppone, *Soft Matter*, 2014, **10**, 2926–2937.
26 G. S. Gopika, P. M. H. Prasad, A. G. Lekshmi, S. Lekshmypriya, S. Sreesaila, C. Arunima, M. S. Kumar, A. Anil, A. Sreekumar and Z. S. Pillai, *Mater. Today: Proc.*, 2020, **46**, 3102–3108.
27 Y. J. Lu, Q. Deng, D. P. Hu, Z. Y. Wang, B. H. Huang, Z. Y. Du, Y. X. Fang, W. L. Wong, K. Zhang and C. F. Chow, *Chem. Commun.*, 2015, **51**, 15241–15244.
28 J. D. McGhee and P. H. von Hippel, *J. Mol. Biol.*, 1974, **86**, 469–489.
29 X. Meng, L. Wang, Y. Zhai and H. Duan, *Res. Chem. Intermed.*, 2020, **46**, 5517–5533.
30 E. E. Rastede, M. Tanha, D. Yaron, S. C. Watkins, A. S. Waggoner and B. A. Armitage, *Photochem. Photobiol. Sci.*, 2015, **14**, 1703–1712.
31 S. B. Howerton, A. Nagpal and L. D. Williams, *Biopolymers*, 2003, **69**, 87–99.
32 Z. Zhang and S. Achilefu, *Org. Lett.*, 2004, **6**, 2067–2070.